POLITECNICO DI TORINO
Repository ISTITUZIONALE

Key Generation of Biomedical Implanted Antennas Through Artificial Neural Networks

(Article begins on next page)

19 April 2024

Key Generation of Biomedical Implanted Antennas Through Artificial Neural Networks

Lida Kouhalvandi
Dept. Electrical and Electronics Engineering
Dogus University
Istanbul, Turkey
lida.kouhalvandi@ieee.org

Ladislau Matekovits
Dept. Electronics and Telecommunications
Politecnico di Torino
Turin, Italy
ladislau.matekovits@polito.it

Ildiko Peter
Faculty of Engineering and Information Technology
University of Medicine, Pharmacy, Science and Technology "George Emil Palade"
Târgu-Mureş, Romania
ildiko.peter@umfst.ro

Abstract—This paper presents an accurate and efficient optimization-based approach for modelling and sizing implanted antennas automatically. The proposed method employs the long short-term memory (LSTM) artificial neural network (ANN) for predicting the design specifications in not only one frequency but also in a large frequency band. The entire process is performed in an automated environment that is the combination of electronic design automation (EDA) tools and the numerical analyzer. Based on this intelligent method, the difficulty of designing electromagnetic (EM)-based antennas is solved to the most degrees and the design parameters can be achieved in the easiest way. To validate the efficiency of the presented ANN, two implanted antennas are designed; they and realized on a grounded biocompatible substrate and covered by bone, muscle, fat, and skin tissues, respectively. These implanted antennas are optimized in terms of input scattering parameter, E-plane and H-plane radiation pattern (RP) specifications and the suitable design parameters are provided automatically. The modelled implanted antennas are appropriate to be used at the industrial, scientific, and medical (ISM) frequency band between 2.4 GHz and 2.5 GHz.

Index Terms—Automated design, artificial neural network (ANN), bandwidth, implanted antenna, long short-term memory (LSTM) layer, radiation pattern (RP).

I. INTRODUCTION

Implanted antennas that can be used in-body communications, play an important role in human's modern daily life and are typically used for health monitoring [1]. These devices can be either receivers or transmitters in body-centric wireless networks; hence, the implanted devices must have appropriate input/output specifications to well-affect the performance of the whole network [2]. Hence, advanced approaches are required for designing high performance implanted antennas.

Basically, the design processes can be classified into either knowledge-based approaches or optimization-based approaches that include equation-based, simulation-based, and learning-based methods. Traditionally, equation-based or simulation-based methods suffer from complex antenna con-figurations and time-consuming simulations. Hence, conventional electronic design automation (EDA) tools need advanced and additional assistance for designing high performance radio frequency designs [3].

Recently, learning-based approaches that include artificial neural network (ANN) have attracted the attention of antenna designers due to their efficient modeling and flexibility which permits to deal numerically with large amount of dataset [4], [5]. Training and constructing an ANN that is modeling the implanted antennas accurately is a big challenge that must be considered carefully and substantially [6]. In configuring the ANN, the definitions of input and output layers are important and even more significant is the construction of the hidden layer that is located between the input and output layers.

In this paper, the ANN technique is employed for designing and optimizing implanted antennas in an effective way. Two implanted antennas in the shape of rectangular and ellipse that are suitable for biomedical applications at the industrial, scientific, and medical (ISM) frequency band of 2.4 GHz- 2.5GHz, are designed. The biomedical tissues as bone, muscle, fat and skin are placed over the antennas where the used substrate is optimized to be titanium dioxide (TiO_2). Employing the ANN with long short-term memory (LSTM) layer makes it significantly important for optimizing the output responses of antenna in a wide frequency band. The entire electromagnetic (EM)-based optimization process is performed automatically, resulting in optimal design parameters with multi-objective output specifications in terms of input scattering parameter (S_{11}), E-plane and H-plane radiation patterns (RPs). The modeling and optimization processes are performed with the combination of an EDA tool as Microwave Studio (Dassault Systèmes) and a numerical analyzer as matrix laboratory (i.e., MATLAB).

This paper is organized as follows: Section II presents the theory of optimization process for modeling and sizing the implanted antennas. Section III describes the simulation results
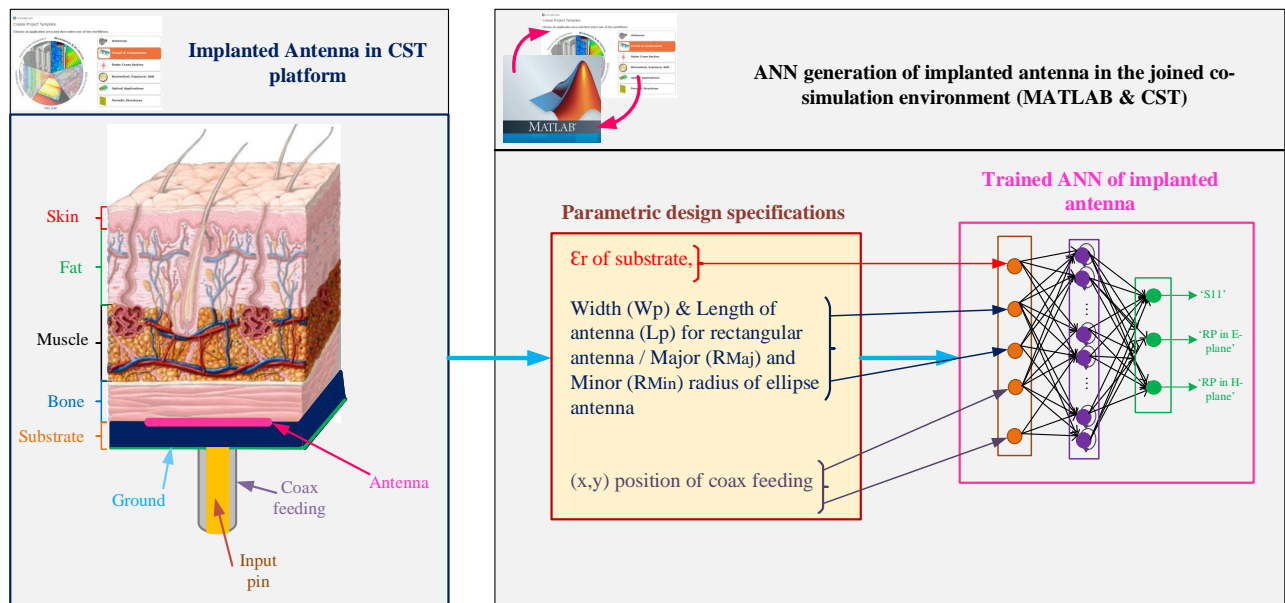
Fig. 1. A comprehensive overview of modeling and sizing the implanted antennas.

and output responses of the optimized implanted antennas. Finally, Sec. IV concludes this paper.

II. ANTENNA DEVELOPMENT

This section provides brief descriptions of the ANN implementation for modeling and sizing the implanted antennas. Firstly, the structure and the configuration of the implanted antenna are described. Then, the automated ANN based method that is employed for sizing the implanted antennas in terms of S_{11} and RPs is explained explicitly. Figure 1 presents the comprehensive knowledge of constructing the implanted antenna by placing the antenna below (embedded in) the biological tissues and also by using ANN technique for sizing them.

A. Construction of implanted antennas

Implanted antennas are important components that can be used inside the human body including the head of humans. Hence, biomedical tissues consisting of bone, muscle, fat, and skin layers must be also considered in the design and simulation process. In this case, the antennas with an optimal and suitable substrate are covered by these biological tissues results in implanted antenna configurations that can be used in biomedical applications. The planner implanted antennas can be developed, for example, in EDA environments such as the Microwave Studio (Dassault Systèmes) [7], or Ansys HFSS [8].

B. ANN technique and it's development

After designing the implanted antennas in the EDA environment, the suitable and optimal design parameters must be determined. In this case, we prefer using the ANN technique for achieving suitable output specifications for the implanted antennas. This technique is selected due to its powerful performance in predicting and optimizing high dimensional designs [9].

Constructing the ANN for the implanted antennas requires special keys including the dataset generation and the definition of input layer, hidden layer, and output layer. The detailed descriptions for training the ANN and Fig. 2 which presents the overall flowchart and demonstrates the use of ANN in implanted antenna designs follows (at the end of this section).

1) Dataset generation: The crucial task for training the ANN is collecting and gathering the appropriate dataset. At the initial phase, two different environments for: i) achieving the EM-based simulation results of implanted antennas and ii) analyzing the large amount of data, are required substantially. Here, we employ the CST Microwave Studio for accessing three specifications as: S_{11}, E-plane, and H-plane RPs, respectively. Also, the MATLAB tool is used to mathematically analyze the data transferred from the CST environment. This process provides the co-simulation environment between CST and MATLAB.

After arranging the simulation and analyzing environments, it is time for generating the dataset. In this case, some/all design parameters of the implanted antenna are selected by the designer then range sweep of each variable is defined in the MATLAB environment. With respect to the defined range, the numerical solver is run, and the implanted antenna's output specifications are assembled in MATLAB. Hereby, as much as data is collected to that degree the ANN is trained and constructed accurately.

2) Definition of ANN's layers: As previously described, any ANN consists of three important layers: an input layer, a hidden layer, and an output layer. Providing features, the number of hidden layers with neurons plays an important role in constructing an accurate ANN.
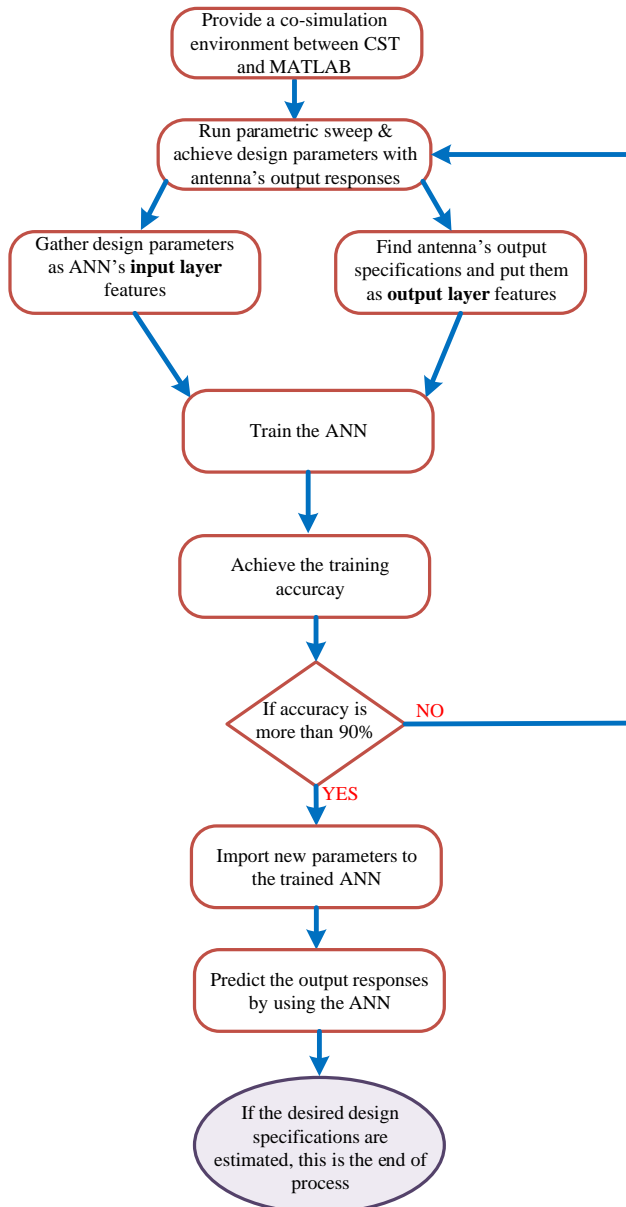
Fig. 2. A general flowchart for sizing the implanted antennas using the ANN.

In this paper, we attempt to design and optimize two implanted antennas of rectangular and ellipse shape, sequentially. Therefore, input layer features are selected due to a determined antenna shape. For our problem, we define input layer features as: relative permittivity (ε_r) of substrate, width and length of patch for rectangular antenna (W_p, L_p), major and minor radius of patch for ellipse antenna (R_{Maj}, R_{Min}), and distance of feeding in the x and y directions (d_x, d_y) (with respect to the center of the radiators).

For the output layer three features are determined as: S_{11}, E-plane, and H-plane RPs. The hidden layer consists of one LSTM layer with determined optimal neuron numbers by the *rule of thumb* theory. The LSTM layer for estimating antenna's output specifications in a large bandwidth and also some single frequency points is selected.

3) Training the ANN: While generation and construction of dataset and ANN's layers are completed, the ANN can be trained. Hereby, input layer features (X_{Train}) and output layer features (Y_{Train}) are applied to (1) for training and constructing the ANN in the MATLAB environment.

$$ \text{net} = \text{trainNetwork}(X_{Train}, Y_{Train}, \text{layers}) \qquad (1) $$

After training the network, its accuracy must be determined. Hence, other input and output dataset namely as X_{Test} and Y_{Test} are assembled in the co-simulation environment. Then, the X_{Test} is inserted into the trained network in (1) and output responses are predicted (Y_{Pred}) with (2). The accuracy is calculated with the difference derivation between the Y_{Pred} and Y_{Test}.

$$ Y_{Pred} = \text{predict}(\text{net}, X_{Test}) \qquad (2) $$

III. SIMULATION RESULTS

This section provides the simulation results of two implanted antennas that are modelled and sized using the ANN technique. Figure 3 depicts the practical implementation of implanted antennas with two different rectangular and ellipse shapes, that are fed by the coaxial cable.
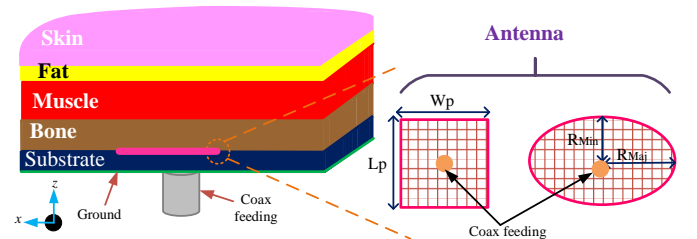

Fig. 3. Configuration of implanted antennas that are modeled using the ANN; (width and length are in mm; drawing not in scale).

In this paper, we use the bone cortical, muscle, fat, and dry skin tissues and place them over the planner antenna. The ε_r and loss tangent ($\tan \delta$) values of various implanted tissues in the large bandwidth of 1 GHz to 10 GHz are provided by refereeing to the [10] and depicted in Fig. 4.

As explained in Sec. II, after constructing the general antenna configuration, the ANN is employed for sizing the design parameters and achieving high performance implanted antennas. Hence, the ANN is trained by defining the input layer and output layer features as Fig. 1 explains. The hidden layer includes a LSTM layer with 100 neurons that are achieved using the rule of thumb. The design parameters, predicted by the ANN, that result in suitable implanted antennas at the ISM frequency band of 2.4 GHz to 2.5 GHz are summarized in Tab. I. It must be noted that both implanted antennas are centered at (0,0) position in the CST designs.

Figure 5 shows the S_{11} performance of two implanted antennas i.e., rectangular and ellipse shapes, at the centered frequency of 2.45 GHz with extension of the ground plane of 18 mm × 16 mm.
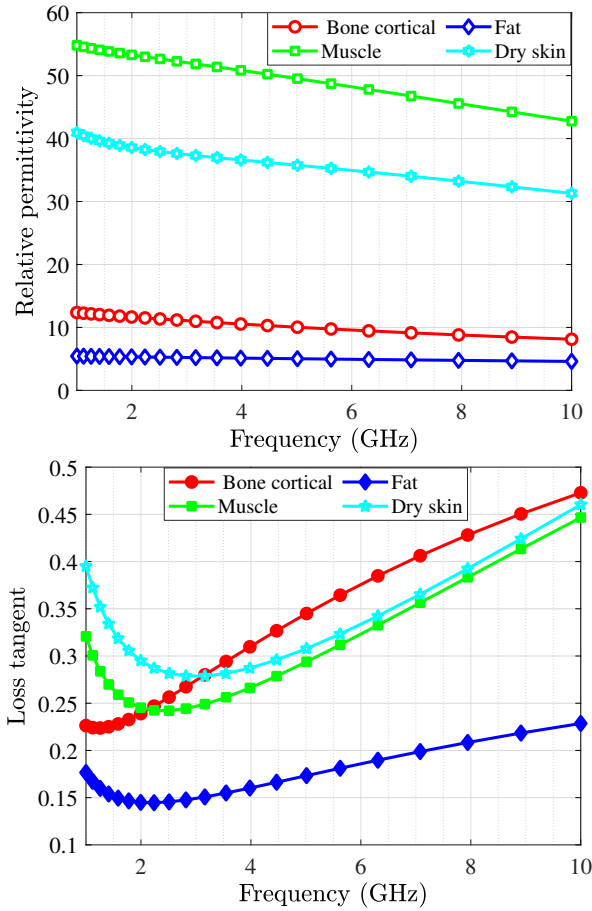
Fig. 4. Relative permittivity (top) and loss tangent (down) of various tissues include bone cortical tissue, muscle, fat, and of dry skin tissues.

TABLE I
OPTIMIZED DESIGN PARAMETERS FOR BOTH IMPLANTED ANTENNAS
USING THE ANN

Design parameters	Value
ε_r	95 (TiO$_2$)
W_p (mm)	4.70
L_p (mm)	7.70
R_{Maj} (mm)	6
R_{Min} (mm)	4.5
d_x (mm)	-1.4
d_y (mm)	0.5 for rectangular and 0.4 for ellipse antennas

Additionally, the RPs in the E-plane and in the H-Plane for both implanted antennas at lower frequency (2.4 GHz), center frequency (2.45 GHz), and upper frequency (2.5 GHz) are shown in Fig. 6. Besides, Tab. II presents the detailed RPs for the rectangular-shaped implanted antennas. The offset of the location of the feeding point(s) - see data in Tab. I (d_y) - does not significantly affect the symmetry of the radiation pattern in the H plane, that instead is more accentuated in the E plane (in Fig. 6). The effect of the finite ground plane is visible in both planes. Similar conclusions can be derived in the case of the elliptic radiators (results not reported).
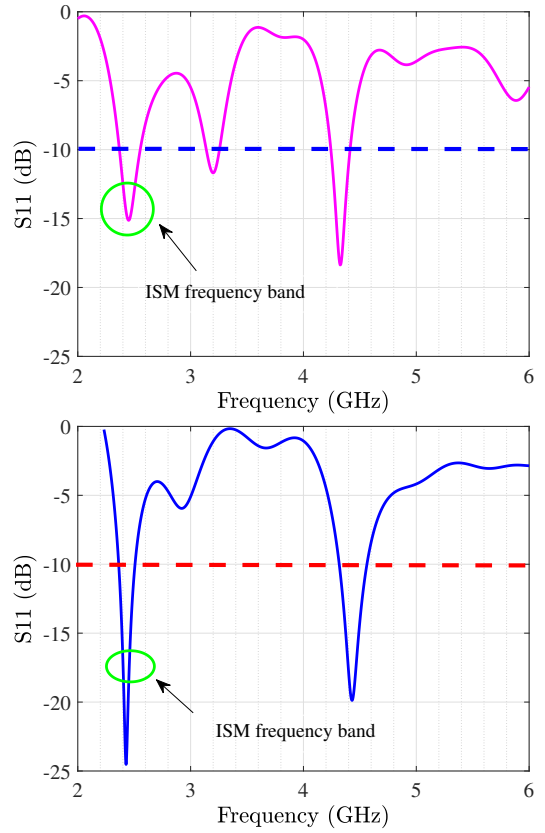

Fig. 5. Input scattering parameter S$_{11}$ of rectangular-shape (top) and ellipse-shape (down) implanted antennas.
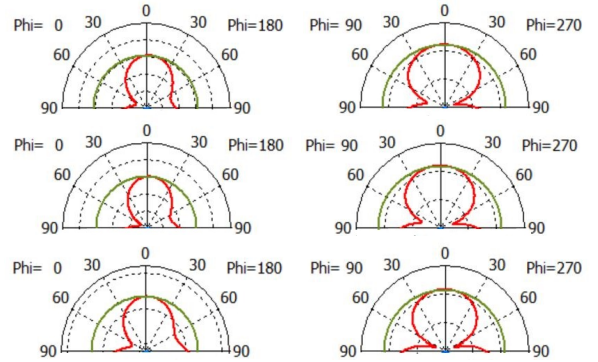

Fig. 6. Radiation pattern of the rectangular antenna in the E- (left) and H- (right) planes at 2.4 GHz (top), 2.45 GHz (middle), and 2.5 GHz (bottom).

IV. CONCLUSION

This paper demonstrates the key benefits of intelligent techniques (i.e., ANN) for modeling and sizing the implanted antennas. The design of implanted antennas, due to the use of various biomedical tissues such as bone, muscle, fat, and skin is not straightforward and is time consuming. Hence, the ANN helps the antenna engineers to design the implanted antennas more easily and without depending from any designer's experience. In this work, the implanted antennas are optimized in terms of three specifications, such as: S$_{11}$, E-plane and H-

TABLE II
OUTPUT RP SPECIFICATIONS FOR RECTANGULAR-SHAPED IMPLANTED
ANTENNA

Rectangular-shaped implanted antenna	2.4 GHz		2.45 GHz		2.5 GHz	
	E-plane	H-plane	E-plane	H-plane	E-plane	H-plane
Main lobe magnitude (dBi)	-4.9	-4.91	-4.49	-4.5	-4.16	-4.18
Main lobe direction (degree)	0	0	0	0	0	0
Angular width (3dB) (degree)	117.9	100	117.4	103.4	117.3	107

plane radiation patterns. Additionally, in the proposed ANN these devices can be optimized in a wide bandwidth, in the light of an LSTM layer. The entire optimization process is performed automatically without any human interruptions and has important results in efficient implanted antenna designs.

ACKNOWLEDGEMENT

REFERENCES

[1] M. M. Soliman, M. E. H. Chowdhury, A. Khandakar, M. T. Islam, Y. Qiblawey, F. Musharavati, and E. Zal Nezhad, "Review on medical implantable antenna technology and imminent research challenges," *Sensors*, vol. 21, no. 9, 2021. [Online]. Available: https://www.mdpi.com/1424-8220/21/9/3163

[2] Q. H. Abbasi, M. U. Rehman, K. Qaraqe, and A. Alomainy, *Advances in Body-Centric Wireless Communication: Applications and State-of-the-Art*, 1st ed. Institution of Engineering and Technology, 2016.

[3] F. Mir, L. Kouhalvandi, L. Matekovits, and E. O. Gunes, "Automated optimization for broadband flat-gain antenna designs with artificial neural network," *IET Microwaves, Antennas and Propagation (in press)*, vol. 10.1049/mia2.12137, 2021.

[4] S. D. Campbell, R. P. Jenkins, P. J. O'Connor, and D. Werner, "The explosion of artificial intelligence in antennas and propagation: How deep learning is advancing our state of the art," *IEEE Antennas and Propagation Magazine*, vol. 63, no. 3, pp. 16–27, 2021.

[5] M. O. Akinsolu, K. K. Mistry, B. Liu, P. I. Lazaridis, and P. Excell, "Machine learning-assisted antenna design optimization: A review and the state-of-the-art," in *2020 14th European Conference on Antennas and Propagation (EuCAP)*, 2020, pp. 1–5.

[6] Y. Sharma, H. H. Zhang, and H. Xin, "Machine learning techniques for optimizing design of double t-shaped monopole antenna," *IEEE Transactions on Antennas and Propagation*, vol. 68, no. 7, pp. 5658–5663, 2020.

[7] "CST Studio suite," http://3ds.com, accessed: 2021-06-21.

[8] "Ansys HFSS," http://ansys.com, accessed: 2021-06-21.

[9] C. Cadir, O. A. Kati, and S. Dumanli, "Matching medium design for in-body communications using artificial neural networks," in *2021 15th European Conference on Antennas and Propagation (EuCAP)*, 2021, pp. 1–5.

[10] "Calculation of the dielectric properties of body tissues," http://niremf.ifac.cnr.it/tissprop/htmlclie/htmlclie.php, accessed: 2021-06-21.